Polymer Chemistry

ROYAL SOCIETY OF CHEMISTRY

PAPER

View Article Online
View Journal

Cite this: DOI: 10.1039/d5py00586h

Polymeric toroidal assemblies formed from ionic homopolymers with shackling photo-responsive behavior

Qingqing Yang,[a] Junjun Lv,[a] Jinye Wang,[a] Wei Song [b] and Liang Ding *[a]

Received 11th June 2025,
Accepted 24th July 2025

DOI: 10.1039/d5py00586h

rsc.li/polymers

The uniformity of toroidal nanostructures and their tunable ring sizes give them promise for applications in many fields, but their synthesis remains challenging. Herein, polyolefin-based homopolymers with pyridinium cation junctions between the main chain and alkyl azobenzene pendant groups were systematically synthesized and self-assembled into preformed spheres due to the solvophobic backbone and electrostatic and strong non-covalent aromatic–aromatic interactions present in the homopolymers. Subsequently, UV light-triggered shackling of the *trans* → *cis* photoisomerization transition was demonstrated, and subsequently, uniform toroids with stable shapes and adjustable dimensions were observed after continuously irradiating with UV light to eventually reach the photostationary state. A mechanistic investigation further confirmed that the strong non-covalent interactions generated during the significantly confined photoisomerization process are essential for the formation of the polymeric toroids. Importantly, the toroidal morphology is not susceptible to the solvent system used, but the ring size can be optionally adjusted from the nanoscale to the microscale by varying other factors. We expect that the importance of the regulation of the different non-covalent interactions in reinforcing each other will offer a new avenue to induce self-assembly of homopolymers to produce uniform and specific morphologies.

Introduction

Amphiphilic block copolymers are well-known to self-assemble into a large variety of micellar nanostructures due to phase separation between their solvophilic and solvophobic segments, and thus they are useful in many applications.[1–3] Of these micellar nanostructures, polymeric toroidal micelles (ring-shaped cylinders or hollow disks) are a relatively rare but fascinating example because their unique geometry is very important for understanding complex biological processes and nanotechnologies.[4–13] Typically, polymeric toroids can be formed by direct polymer self-assembly[14–16] and the indirect morphology transition of assemblies, or by the disassembly of hierarchical structures.[17–20] Most known toroidal micelles are formed based on the latter route *via* end-to-end coalescence. However, these toroidal nanostructures always coexist with other morphologies. Recently, direct polymer self-assembly for the formation of toroidal assemblies has drawn extensive attention because it is facile to conduct and because of the diversity of products it gives. Importantly, pure toroidal assemblies can be obtained by controlling the self-assembly conditions.[21–23] Nonetheless, the rapid and facile preparation of toroids of uniform and tunable ring size remains a challenge in the field of polymer self-assembly.

Different from the relatively sophisticated synthesis and self-assembly process of amphiphilic block copolymers, homopolymer assemblies usually have enhanced stability and diversity that are attributed to their ambiguous solvophilic–solvophobic boundary and special self-assembling driving force.[24] The main strategies for the preparation of homopolymer assemblies can be classified into two categories—the polymerization of elaborately designed amphiphilic monomers,[25–29] and the self-assembly of solvophilic homopolymers induced by solvophobic end-groups.[30–34] The most obvious similarity between the two distinct approaches is that non-covalent interactions must be considered first, as it is the driving force in the design of nanostructured macromolecules and the formation of assemblies with desirable morphologies.

Generally, non-covalent interactions comprise hydrogen bonding, π–π stacking, electrostatic forces, metal–ligand coordination, charge-transfer, *etc*. By synergizing two or more non-covalent bonding interactions to enhance the intra- or intermolecular interactions in homopolymer assemblies and further control them in a suitable range, unique nano-

[a]*State Key Laboratory for Chemistry and Molecular Engineering of Medical Resources, School of Chemistry and Pharmaceutical Sciences, Guangxi Normal University, Guilin, 541004, China. E-mail: dingliang1984@gxnu.edu.cn*
[b]*Department of Polymer and Composite Material, School of Materials Science and Engineering, Yancheng Institute of Technology, Yancheng, 224051, China*

structures, including polymeric toroids, can be formed through homopolymer self-assembly.[35–37] Furthermore, the strength of the assemblies changes when one type of non-covalent interaction reinforces or weakens the other, ultimately enabling access to remarkable variations in self-assembly morphology and physicochemical properties.[38–40] Even so, research focusing on homopolymer self-assembly remains limited—presumably due to challenges in monomer design, unpredictable self-assembly behavior, difficulty in forming uniform and size-tunable morphologies, and, in particular, the complexity of modulating non-covalent interactions. Furthermore, during the process of self-assembly, non-covalent interactions significantly rely on the external environmental conditions, such as temperature, light, pH, solvent polarity, the concentration and molecular weight of the homopolymer,[41–45] thus providing the opportunity to promote the scope of structure fine-tuning. Among these stimuli, light is a non-interventional factor that has been widely used in the structure and property transformation of light-responsive homopolymer systems, and it also allows control over the shape, size, and microstructure of assemblies.[46,47] Thus, it is important to establish the effect of light irradiation on the regulation of non-covalent interactions, manipulating the self-assembly process, and the formation of toroidal homopolymer assemblies.

Based on the above facts, we fabricated a novel self-assembly system based on a light-responsive homopolymer containing a charged pyridinium bromide junction group between the polyolefin backbone and solvophobic alkyl azobenzene (azo) pendant. This structure creates ionic bonding interactions and strong non-covalent aromatic–aromatic interactions, further promoting the formation of highly ordered structures which drive the homopolymers to self-assemble into the preformed assemblies. Under continuous UV-light irradiation, the utilization of electrostatic forces to reduce the mobility of pendant groups further restricts the ability of the azo chromophores to undergo photoisomerization transition, thus enhancing the aromatic–aromatic interactions of the photostationary state and eventually achieving a controllable evolution to form toroidal nanostructures with uniform morphologies and tunable sizes (Scheme 1). Thereby, the realization of homopolymer assemblies was mainly ascribed to the presence of multiple non-covalent interactions, while the generation of pure toroids was attributed to UV light-triggered shackling-photoisomerization behavior.

Results and discussion

Synthesis of ionic azo-monomers and ADMET polymerization

The preparation of azo-functionalized ionic polyolefins requires only one criterion—the design of suitable ionic α,ω-dienes without any trace impurities. Herein, ionic azo-monomers, **IAzoC$_p$Ms** (p = 0, 3) were synthesized *via* a simple protocol in two steps from commercially available starting materials to afford a bromopropyl-diene, followed by exhaustive reaction with excess azo-pyridine compounds to obtain the desired diene monomers (Scheme S1). Afterwards, our investigations began with the optimization of the reaction conditions of the ADMET polymerization of **IAzoC$_p$Ms** along with 0.5 mol% Grubbs second-generation catalyst. The reaction was easily completed in 24 h to produce the pendant ionic azo-homopolymers, **IAzoC$_p$HPs**. ^{1}H NMR spectra and GPC traces of all compounds, **IAzoC$_p$Ms** and **IAzoC$_p$HPs**, are provided in Fig. S1–S12 to confirm their chemical structures. Additionally, the detailed characteristics of **IAzoC$_p$HPs** are summarized in Table 1, which displays the relatively moderate molecular weights (M_n ~20 kDa) and distribution indices ($Đ$ ~1.70), thus demonstrating the successful synthesis of **IAzoC$_p$HPs**.

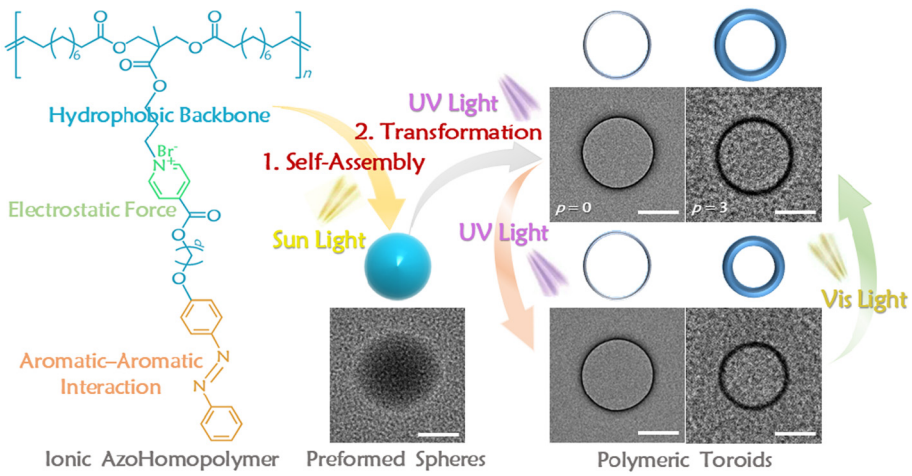

Scheme 1 Evolution from ionic preformed azo-homopolymer spheres to polymeric toroids based on the synergy of a solvophobic backbone, electrostatic forces, and aromatic–aromatic interactions triggered by UV light-induced shackling *trans* → *cis* isomerization of the azo pendant groups. Scale bar: 100 nm.

Table 1 Synthesis, characteristics and photoisomerization transition data of **IAzoC$_p$HPs**

Homopolymer[a]	$M_{n,GPC}$ [b] (kDa)	$Đ$[b]	$\lambda_{0,max}$ [c] (nm)	(Back)-isomerization efficiency[d] (%)	k_i [e] ($S^{-1}/10^{-2}$)	k_r [f] ($S^{-1}/10^{-2}$)
IAzoC$_3$HP	18.5	1.72	331	24.3 (98.6)	0.52 ± 0.02	0.92 ± 0.02
IAzoC$_0$HP	19.8	1.69	319	12.9 (98.8)	0.41 ± 0.01	0.80 ± 0.03

[a] Reaction conditions: [**monomer**] : [**catalyst**] = 100 : 1, and [**monomer**] = 1.0 mol L^{-1} for ADMET polymerization at 70 °C for 24 h. [b] The molecular weights and distribution indexes of the **IAzoC$_p$HPs** homopolymers were determined by GPC using DMF as the eluent. [c] The maximum absorption wavelength in the original state for the sample solution. [d] Calculated using the formula $(A_0 - A^{trans\rightarrow cis})/A_0$, where $A^{trans\rightarrow cis}$ is the maximum absorbance of the sample solution after UV-light irradiation to reach a PSS. A_0 is the maximum absorbance of the sample solution in the original state. The ratio of $A^{cis\rightarrow trans}/A_0$, $A^{cis\rightarrow trans}$ denotes the absorbance at the PSS of the visible light-induced *cis* → *trans* back-photoisomerization. [e] The rate constant of the *trans* → *cis* photoisomerization transition. [f] The rate constant of the *cis* → *trans* photoisomerization transition.

Photoisomerization behavior of the ionic azo-homopolymers

Usually, azo-polymer have *trans* and *cis* isomers which show high-intensity π → π* and relatively low-intensity n → π* transition bands located in the UV and visible (Vis) regions, respectively.[48] The configuration of the azo chromophore switched by photoisomerization varies, depending on its position in the polymer chain and the nature of adjacent groups.[49,50] Here, as IAzoC$_p$HPs contain photosensitive azo pendants, it was instructive to examine how adjacent ionic bonding influences the UV–vis absorption properties of the polymers.[51] Therefore, the isomerization behaviors of **IAzoC$_p$HPs** in diluted THF solutions were surveyed in detail using UV–Vis analysis to provide adequate information on the polymer structures and their photoresponsive properties.

For **IAzoC$_0$HP**, which has a pyridinium cation directly connected to the azo unit that is affected by electrostatic forces, the absorption peak of the azo chromophore, ascribed to the π → π* transition of the *trans* isomer, was shifted to around 319 nm. Only about 13% of the *trans* isomer was converted to the *cis* isomer after UV light irradiation at 365 nm and reaching the photostationary state (PSS), and thus **IAzoC$_0$HP** exhibits noticeable photoisomerization suppressing behavior (Fig. 1c). After irradiation with 460 nm visible light the absorbance recovered quickly and more than 98% of the azo moieties had the *trans* configuration (Fig. 1d). Additionally, **IAzoC$_3$HP** displayed similar photoisomerization behavior but with obviously different absorption peaks (Fig. 1a and b) when compared with **IAzoC$_0$HP**. The large hypsochromic shift of **IAzoC$_3$HP** was nearly 12 nm, and the *trans* → *cis* conversion efficiency increased to about 24% at the PSS (Table 1), indicating that the suppression by electrostatic forces on photoisomerization was weakened when there was a methylene spacer between the pyridinium cation junction and the azo pendant.[52,53] Furthermore, the rate constants of the *trans* → *cis* photoisomerization (k_i) and *cis* → *trans* relaxation (k_r) for **IAzoC$_p$HPs** were calculated from the first-order kinetic curves (Fig. S13a and S13b). As summarized in Table 1, the curves were plotted based on the absorbance at 319 and 331 nm corresponding to the π → π* transition in Fig. 1 and according to the linear plots of $\ln[(A_\infty - A_t)/(A_\infty - A_0)]$ *versus* irradiation time.[54] Unlike traditional azo-polymers, the **IAzoC$_p$HPs** had relatively low rate constants, and k_i was lower than k_r, which was in accordance with the shackling of the *trans* → *cis* isomerization. Meanwhile, **IAzoC$_3$HP** had higher rate constants than **IAzoC$_0$HP**, suggesting that the methylene spacer reduced the restriction on photoisomerization. As expected, the photoisomerization of the **IAzoC$_p$HPs** can be mediated reversibly several times through subsequent cycles of UV and visible light irradiation with almost no significant loss in absorbance, thus demonstrating the stability of the polymers in light-responsive applications.[55] Generally, the azo pendant in the *trans* state has a rod-like molecular structure that exhibits strong non-covalent aromatic–aromatic interactions in the rigid arrangement, whereas the *cis* configuration usually has a bent shape with low anisometry and extremely weak π–π interactions.[50] Thus, UV light-driven shackling of the isomerization behavior resulted in polymers with a greater amount of the *trans* configuration that would produce a relatively sufficient number of non-covalent interactions at the PSS to induce the **IAzoC$_p$HPs** to self-assemble and trigger the morphological evolution.

Morphologies of the self-assembled ionic azo-homopolymers

To demonstrate the light-triggered toroid formation, we systematically investigated the effect that the pendant shackling-driven suppression of the photoisomerization behavior had on the self-assembled morphologies. Under continuous irradiation with 365 nm UV light until the PSS was reached, the **IAzoC$_p$HPs** could self-assemble into polymeric toroids in THF with an initial concentration of 0.01 M due to the strong electrostatic forces between the pyridinium cations and the non-covalent aromatic–aromatic interactions of the azo pendants. Interestingly, the formed toroidal nanostructures have different widths depending on the *trans* → *cis* photoisomerization efficiency of the **IAzoC$_p$HPs** at the PSS. However, it was difficult for us to identify the hollow vesicles and polymeric toroids in the SEM images even after using varying initial concentrations (Fig. S14). Afterward, the magnified TEM images were obtained, as shown in Scheme 1, which were consistent with the corresponding toroidal morphologies. As expected, toroidal homopolymer nanostructures were self-assembled from the **IAzoC$_p$HPs** upon continuous exposure to UV light irradiation to eventually reach the PSS.

Specifically, for the **IAzoC$_p$HPs**, polymeric toroids that were highly regular and uniform in shape and size were observed using TEM when the initial concentration was 0.03 M (Fig. 2).

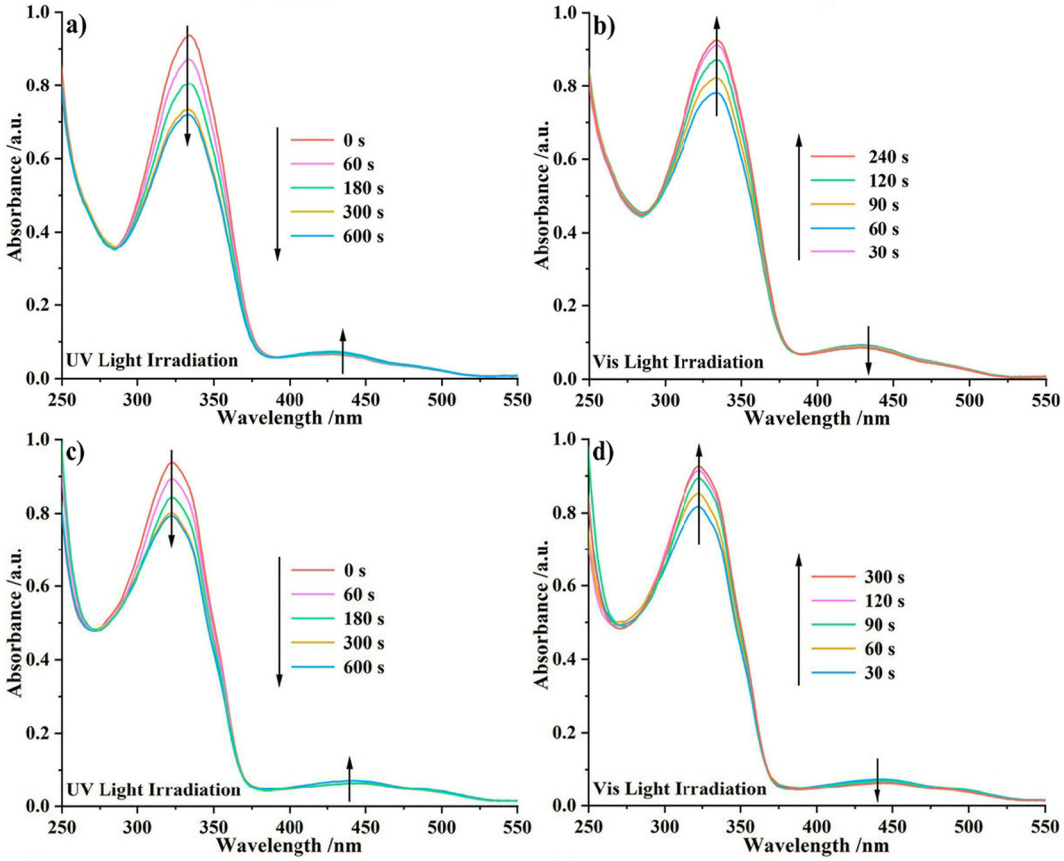

Fig. 1 UV–vis spectra of **IAzoC$_3$HP** (a and b) and **IAzoC$_0$HP** (c and d) in diluted THF solutions at a concentration of 2.5 × 10^{-5} mol L^{-1}. Absorbance changes as a function of UV light and Vis light irradiation times.

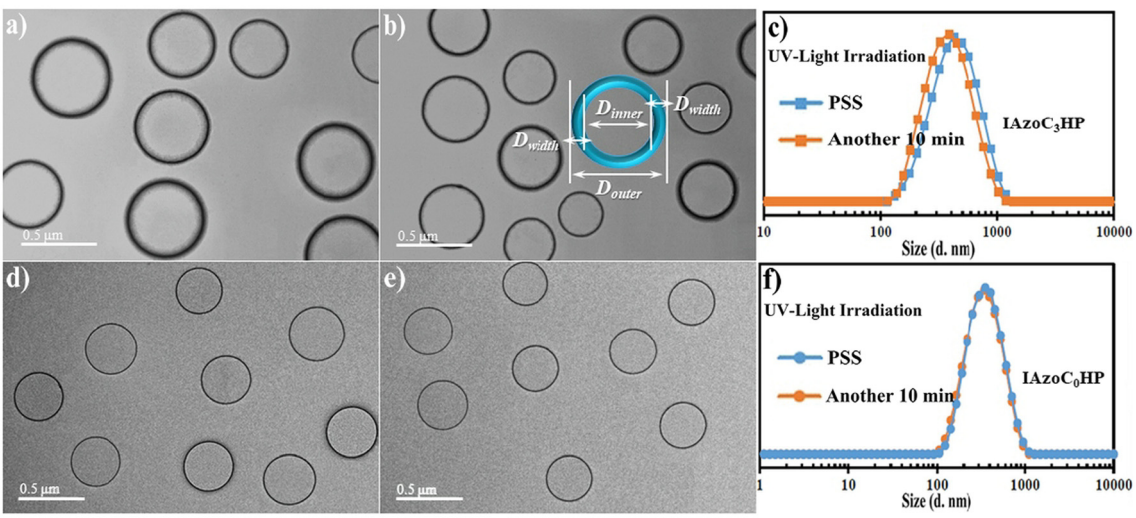

Fig. 2 TEM images and corresponding DLS results of the polymeric toroids self-assembled from (a–c) **IAzoC$_3$HP** and (d–f) **IAzoC$_0$HP** at an initial concentration of 0.03 M after irradiation with UV light to reach the photostationary state and after an extension of the irradiation time for 10 min.

What is more, no other nanostructures were found to coexist with the toroids. By analyzing the representative toroids in Fig. 2a and d, it was noteworthy that the width of the toroid (D_{width} = 42 nm) was evident for **IAzoC$_3$HP** while the average inner diameter (D_{inner}) of the toroid was determined to be 363 nm, which was in accordance with the hydrodynamic dia-

Table 2 Summary of self-assembly behavior of the **IAzoC$_p$HPs** in THF

Homopolymer	$M_{n,GPC}$ (kDa)	$D_{h,DLS}$ [a] (nm)	PDI[a]	$D_{h,TEM}$ [b] (nm)	Concentration (mol L^{-1})
IAzoC$_3$HP	18.5	182	0.158	149 (26)	0.01
		418	0.175	363 (42)	0.03
		552	0.189	456 (67)	0.05
		613	0.195	505 (78)	0.06
		676	0.203	592 (86)	0.075
		865	0.221	717 (129)	0.1
IAzoC$_0$HP	19.8	116	0.139	98	0.005
		165	0.146	153	0.01
		292	0.128	271	0.02
		380	0.142	356	0.03
		457	0.140	442	0.05

[a] *Z*-Averaged hydrodynamic diameter (D_h) and polydispersity determined in THF using DLS. [b] Average inner diameter (D_{inner}) of the **IAzoC$_p$HPs** and the width (D_{width}) of **IAzoC$_3$HP** were determined in THF using TEM.

meter (D_h = 418 nm) measured using DLS (Fig. 2c and Table 2). After irradiation with 365 nm UV light, the ring size decreased slightly (D_{inner} = 347 nm and D_h = 396 nm as shown in Fig. 2b and c), but the width remained unchanged. Conversely, the polymeric toroids derived from the self-assembly of **IAzoC$_0$HP** were thermodynamically stable even under extended UV light irradiation times (D_{inner} = 356 and 352 nm in Fig. 2d–f) or after long storage times (D_{inner} = 364 and D_h = 387 nm after two weeks in Fig. S15). These findings implied that the inner structure of the assemblies barely changed during the photoisomerization process. This special toroidal morphology can be attributed to the continuous enhancement of the non-covalent aromatic–aromatic interactions due to the extremely low isomerization efficiencies (approximately 13% and 24% for **IAzoC$_0$HP** and **IAzoC$_3$HP**, respectively). All these results also demonstrated that an appropriately sized methylene spacer between the pyridinium

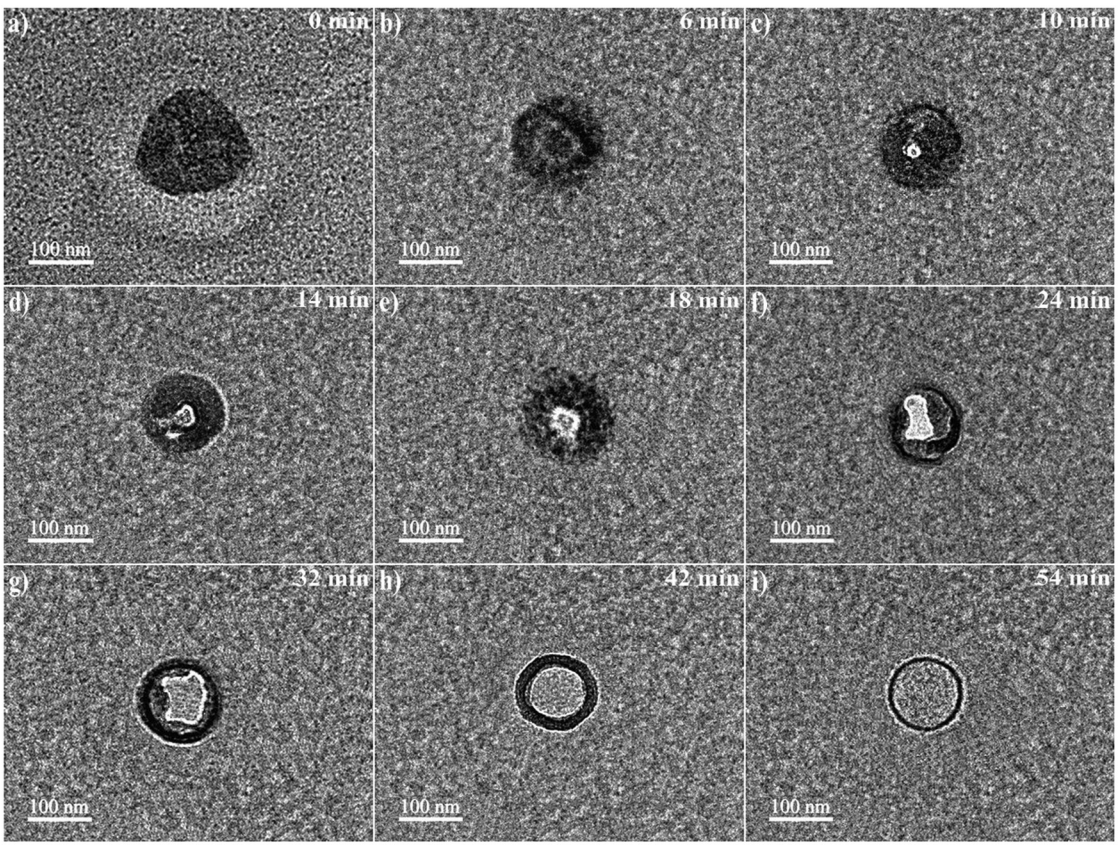

Fig. 3 TEM images show the morphological evolution of the toroids derived from **IAzoC$_0$HP**. Under UV light irradiation for different times until the photostationary state was reached, a preformed sphere is formed (a), followed by a complex micelle (b), a semi-vesicle (c–f), a hollow vesicle (g), a polymeric toroid with a specific width (h), and toroidal assemblies (i).

cation junction and azo pendant in **IAzoC$_p$HPs** was critical for suppressing the *trans* → *cis* isomerization transition to form the toroidal nanostructures.

Polymeric toroid formation mechanism

In our previous study, we detected a shackling photoisomerization phenomenon, in which UV light was used as the driving force to induce non-amphiphilic polymer self-assembly and trigger morphological evolution.[52] Therefore, we wondered what would happen if the self-assembly of the **IAzoC$_p$HPs** was carried out without UV light irradiation, as the azo units in the formed assemblies are mainly in the *trans* configuration with strong non-covalent aromatic–aromatic interactions that are kinetically controlled. To obtain a deep insight into the formation mechanism of the toroidal morphologies from the **IAzoC$_p$HPs**, as a model system, a diluted **IAzoC$_0$HP** THF solution (0.005 M) was selected and self-assembled in sunlight first. Accordingly, the fully extended homopolymer chains in THF shrank and aggregated to produce spherical assemblies that gradually transformed into polymeric toroids after continuous UV light irradiation to minimize the free energy of the system. As shown in Fig. 3, for a comprehensive understanding of toroid formation, the kinetic evolution process triggered by UV light-induced shackling of the *trans* → *cis* isomerization was visualized through TEM images obtained at different irradiation stages.

Before UV-light irradiation, the preformed spheres were distinctly observed (Fig. 3a) due to the solvophobic nature of the soft polyolefin backbone, the electrostatic forces from the pyridinium cation junction, and the strong aromatic–aromatic interactions between the *trans* isomers of the rigid azo units. Based on the subsequent evolution, we speculate that the neutral polymer main chain and azo pendant form the core and that the charged pyridinium salt protrudes out of the core region into the surrounding phase. After irradiating with UV light for 6 min, the *trans* → *cis* isomerization transition partly disrupted the non-covalent interactions, resulting in homogenous shrinkage to form complex micelles (Fig. 3b). By prolonging the UV light irradiation time to 18 min, the shackling of the isomerization process prompted more *trans*-azo groups to be confined within the sphere-like micelles which enhanced the interactions between the homopolymer chains while hindering further shrinkage. Due to space constraints and energy release, several holes subsequently appeared in the micellar surface and were forced to expand towards the center, leading to the formation of semi-vesicles and hollow vesicles (Fig. 3c–f). As the irradiation time was further increased to

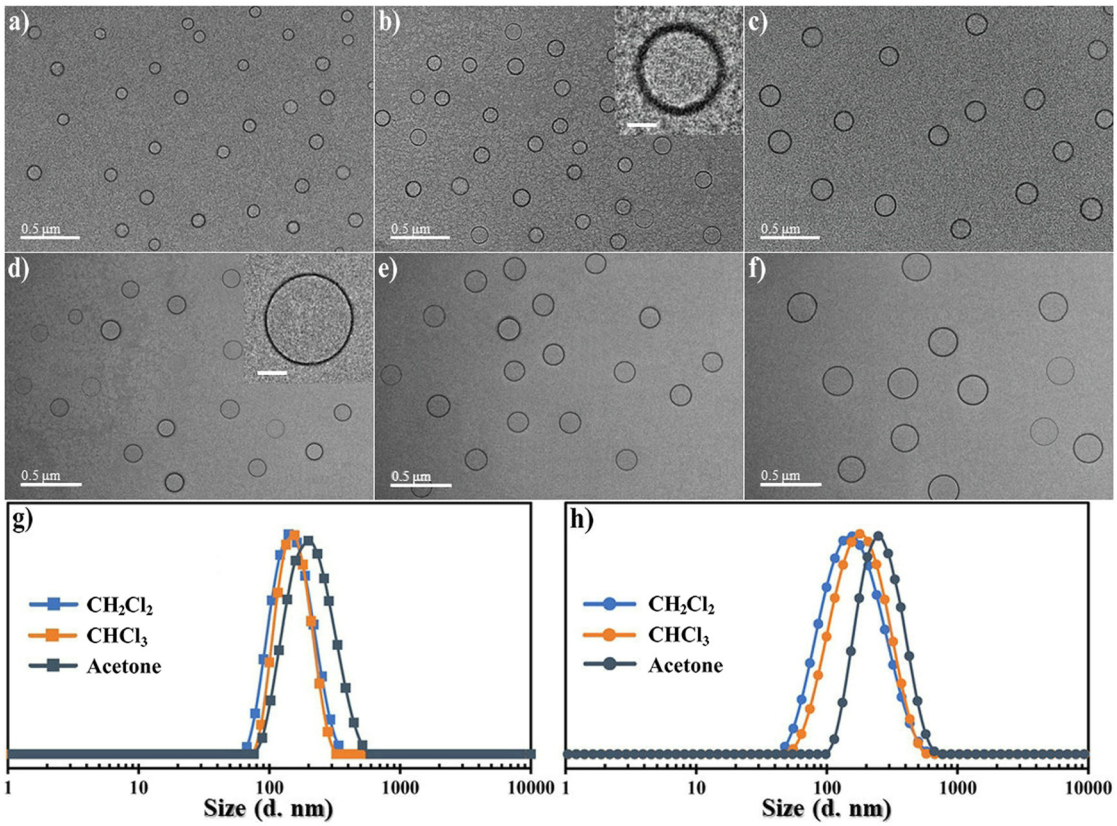

Fig. 4 Self-assembly of (a–c) **IAzoC$_3$HP** and (d–f) **IAzoC$_0$HP** to form polymeric toroids in CH_2Cl_2, $CHCl_3$ and acetone, respectively from left to right, at a concentration of 0.01 M. (g and h) DLS results of the toroids corresponding to the TEM images in (a–c) and (d–f), respectively. All the samples were continuously exposed to UV light. Scale bar in the high-resolution TEM images: 50 nm.

30 min, the spherical vesicles eventually evolved into polymeric toroids (Fig. 3g–i) through a perforation pathway based on dynamic stability and thermodynamic equilibrium.[56] Of course, the micelles, vesicles, and other formations can only be regarded as metastable states of the self-assembly process, and the system evolved *via* different paths from the initial semispherical state to the final toroidal state.

Actually, throughout the whole evolution process, the composition of the morphology remains almost unchanged. Here, the vital factor is the electrostatic forces that constrain the side chain mobility, which then wraps the azo unit inside the nanoaggregate to suppress the *trans* → *cis* isomerization transition and generate more *trans* isomers at the PSS, thus improving the aromatic–aromatic interactions when continuously exposed to UV light. This was further confirmed by DLS analysis (Fig. S16) and fluorescence studies of **IAzoC$_0$HP** (Fig. S17). Therefore, the presence of multiple non-covalent interactions in the polymer is only an essential prerequisite to obtain the well-defined assemblies, while the shackling of the photoisomerization behavior is considered as the main driving force for achieving the self-assembly morphological transformation and acquiring a uniform toroid structure.

Effect of solvent polarity, concentration and molecular weight of the homopolymer on toroid formation

During the self-assembly of the solvophilic homopolymers in an organic solvent/H_2O mixture, in addition to the non-covalent interactions between the solvophobic end-groups, the polar solvent fraction plays an important role in determining the assembled morphologies.[57] Therefore, it is difficult to conveniently construct a uniform toroid while precisely and efficiently tuning the ring size. In this system, the **IAzoC$_p$HPs** directly formed spherical assemblies, first in THF, then evolved to toroidal nanostructures after continuous UV light irradiation. Accordingly, the impact of solvent polarity on the self-assembly is eliminated. To confirm this speculation, solvent-dependent self-assembly experiments of the **IAzoC$_p$HPs** were performed, and the detailed results are summarized in Table S1. As expected, the **IAzoC$_p$HPs** in different solvents (relatively low-polarity CH_2Cl_2, similar-polarity $CHCl_3$, and relatively strong-polarity acetone) at a concentration of 0.01 M exhibited similar tendencies in morphological evolution to those observed in THF, ultimately forming uniform toroidal systems (Fig. 4a–f). Conversely, with a slight increase in solvent polarity, the interaction between the polymer chains improves correspondingly, resulting in polymeric toroids with larger diameters (Fig. 4g and h).

The size of the polymeric toroid can also be adjusted flexibly by switching the self-assembly concentration. Usually, the formation of toroidal assemblies is conducted in a dilute solution.[56] Here, as the concentration of **IAzoC$_0$HP** increased from 0.005 to 0.05 M, the local density of the homopolymer chains was enhanced accordingly, leading to improved electrostatic and π–π stacking interactions that hindered homogenous shrinkage,

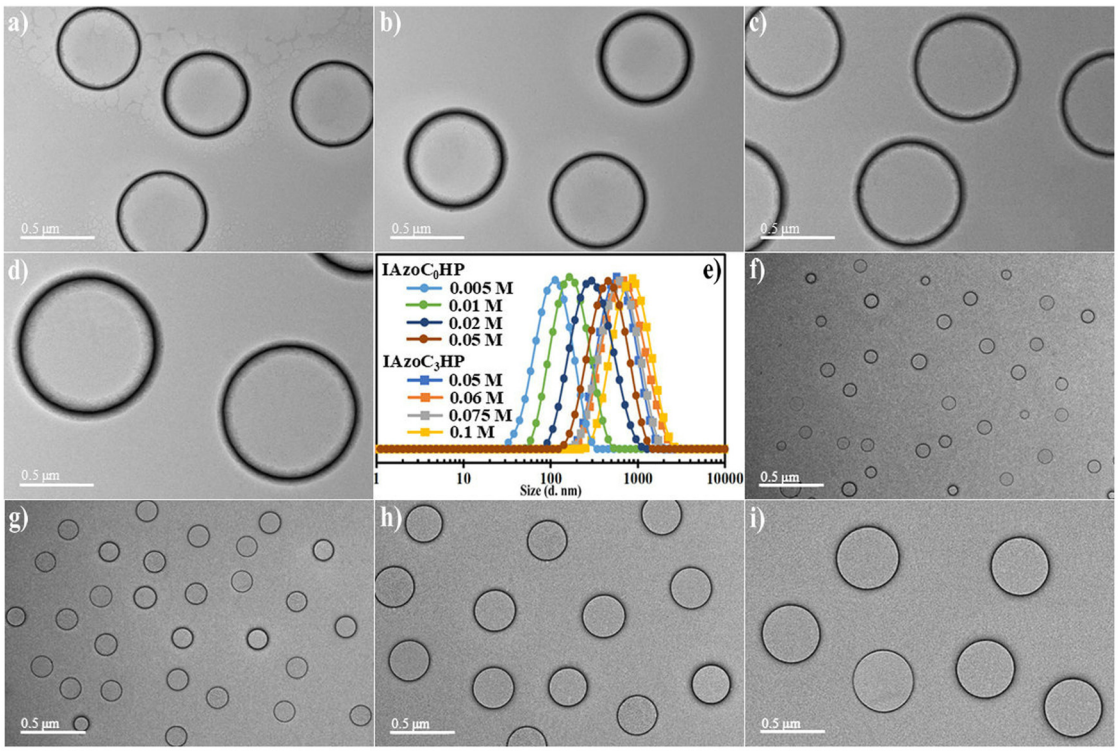

Fig. 5 TEM images and corresponding DLS results of the polymeric toroids with increased sizes self-assembled from (a–e) **IAzoC$_0$HP** at different initial concentrations of 0.005, 0.01, 0.02 and 0.05 M and (e–i) **IAzoC$_3$HP** at different initial concentrations of 0.05, 0.06, 0.075 and 0.1 M after continuously irradiation with UV light.

while accelerating collision and fusion of adjacent toroids, and ultimately the hydrodynamic diameter of the toroids increased from 116 to 457 nm (Fig. 5e). This increase in size allowed the minimization of the local free energy, and the observed sizes were in accordance with the ring sizes measured from the TEM images (Fig. 5a–d and Table 2). Similar self-assembly results for **IAzoC$_3$HP** are demonstrated in Fig. 5e–i, and the details of the sizes are also summarized in Table 2. This is a typical phenomenon where the diameter of the assembly increases linearly with the concentration (Fig. 6, blue lines). Although the process of diameter growth was hard to probe using electron microscopy, insights from the dimensional regulation and toroidal assembly strategy help us propose a possible reason for the concentration-promoted transformation. A high concentration is conducive to

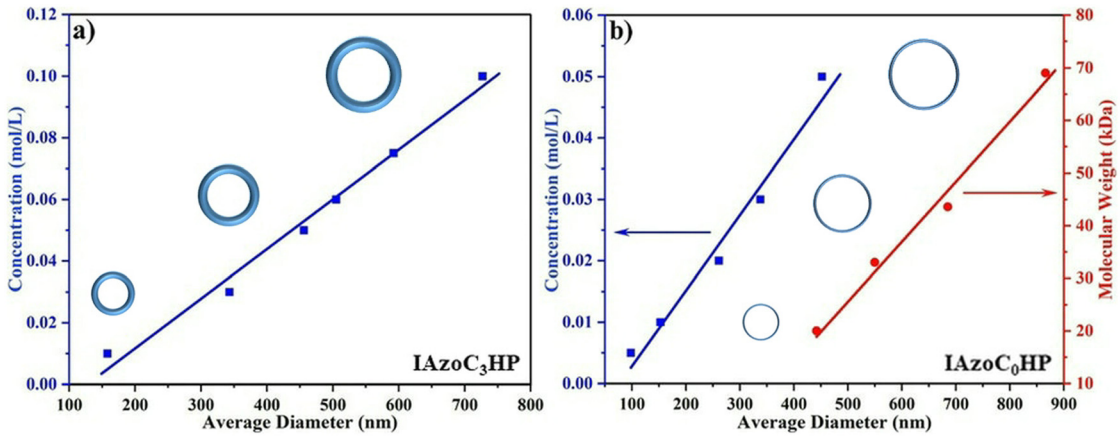

Fig. 6 The relationship between the average diameter of the toroids and the self-assembly concentration of (a) **IAzoC$_3$HP** and (b) **IAzoC$_0$HP** (blue lines) and the molecular weight of **IAzoC$_0$HP** (red line).

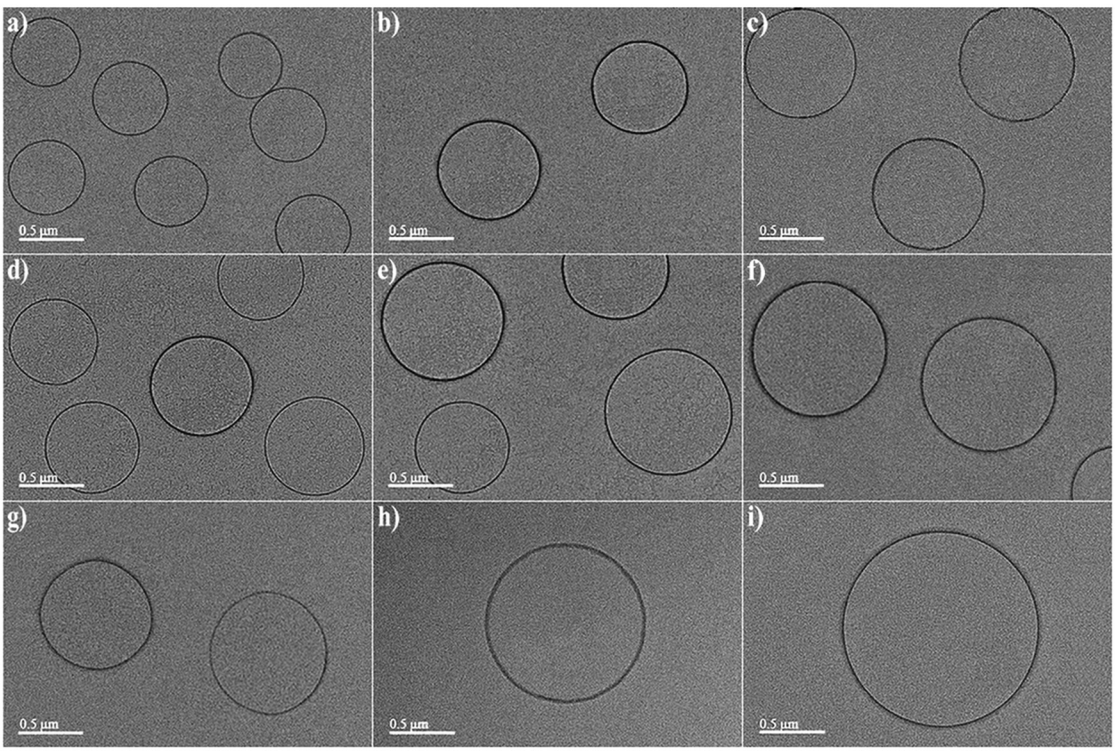

Fig. 7 TEM images of polymeric toroids with increasing sizes formed from different initial concentrations where the molecular weights of the **IAzoC$_0$HPs** are (a–c) 33, (d–f) 42 and (g–i) 69 kDa, respectively. TEM images show the corresponding toroidal nanostructures at 0.05, 0.1 and 0.2 M, respectively from left to right. All the samples were continuously exposed to UV light.

the secondary aggregation of toroids to access a more stable state, whereas at a lower concentration, the polymeric toroids tend to disperse homogeneously. This behavior is different from the assemblies of typical amphiphilic polymers, where the shape and size are usually manipulated by a high polarity solvent ratio.[58]

The dimensions of the polymeric toroids can also be controlled sensibly by varying the molecular weight of the corresponding **IAzoC$_p$HPs**. As shown in Fig. 6, increasing the molecular weight of **IAzoC$_0$HP** to approximately 33, 42, and 69 kDa led to a progressive increase in toroid diameter at an initial concentration of 0.05 M. The corresponding diameters were 558, 705, and 846 nm, respectively (Fig. 7a, d and g). Based on this, the relationship between the average diameter of the toroids and the molecular weight of **IAzoC$_0$HP** is also presented in Fig. 6b (red lines), exhibiting a linear relationship. As the molecular weight of **IAzoC$_0$HP** increases, the non-covalent electrostatic and π–π stacking interactions between the homopolymer chains improve accordingly, which further hinders homogeneous shrinkage in the early stage, leading to the formation of larger toroids. Interestingly, when the initial concentration was further increased to 0.1 and 0.2 M alongside the molecular weight of **IAzoC$_0$HP**, the formation of toroidal assemblies occurred across a broad range of spatial scales, from nanometres (Fig. 7b, c, e and f) to microns (Fig. 7h and i).

Conclusions

In summary, we demonstrated a unique UV light-induced morphological evolution strategy to fabricate uniform toroids. Two types of polyolefin-based homopolymers with a charged pyridinium bromide junction group and alkyl azo pendants were synthesized *via* ADMET polymerization. These homopolymers could further self-assemble into preformed spheres in sunlight, as a result of their multiple non-covalent interactions. Upon UV light irradiation, the *trans* → *cis* isomerization efficiency of the azo unit can be regulated by changing the length of the alkyl side chain, which provides precisely adjustable π–π stacking to convert the preformed spheres into polymeric toroids with stable shapes and fixed sizes. Importantly, the formation of morphologically pure toroids with uniform and tunable ring sizes was independent of the solvent system used. However, the formation process was susceptible to the initial self-assembly concentration and molecular weight of the homopolymer. The mechanism and approach to construct the artificial toroids not only offer a feasible and effective pathway to prepare toroidal assemblies but also provide a new strategy for controlling the self-assembly process and modulating the morphological transformation of assemblies.

Author contributions

Q. Yang and J. Lv synthesized, analyzed, and characterized all compounds, monomers and polymers. J. Wang and W. Song analyzed the morphology and performed the polymer testing and analysis and wrote the discussion. Q. Yang and L. Ding wrote the draft manuscript and all the authors contributed to finalize the manuscript though proofreading. All authors approved the final version of the manuscript.

Conflicts of interest

The authors declare no conflict of interest.

Data availability

Experimental and characterization methods used, the synthetic routes, the ^{1}H NMR spectra, GPC traces, DLS results, TEM images, SEM images, and UV–Vis spectra.

See DOI: **https://doi.org/10.1039/d5py00586h**.

Acknowledgements

The authors thank the National Natural Science Foundation of China (no. 22361006 and 21774107), the Natural Science Foundation of the Jiangsu Higher Education Institutions of China (no. 18KJB430027), Qing Lan Project of Jiangsu Province, and the Initial Scientific Research Foundation of Guangxi Normal University for financial support of this research.

References

1 Y. Mai and A. Eisenberg, Self-assembly of block copolymers, *Chem. Soc. Rev.*, 2012, **41**, 5969–5985.
2 J.-P. Xu and J.-T. Zhu, Block copolymer colloidal particles with unique structures through three-dimensional confined assembly and disassembly, *Chin. J. Polym. Sci.*, 2019, **37**, 744–759.
3 C. K. Wong, X. L. Qiang, A. H. E. Müller and A. H. Gröschel, Self-assembly of block copolymers into internally ordered microparticles, *Prog. Polym. Sci.*, 2020, **102**, 101211.
4 C. C. Conwell, I. D. Vilfan and N. V. Hud, Controlling the size of nanoscale toroidal DNA condensates with static curvature and ionic strength, *Proc. Natl. Acad. Sci. U. S. A.*, 2003, **100**, 9296–9301.
5 Z. Y. Chen, H. G. Cui, K. Hales, Z. B. Li, K. Qi, D. J. Pochan and K. L. Wooley, Unique toroidal morphology from composition and sequence control of triblock copolymers, *J. Am. Chem. Soc.*, 2005, **127**, 8592–8593.
6 Y.-L. Liu, Y.-H. Chang and W.-H. Chen, Preparation and self-assembled toroids of amphiphilic polystyrene-C_{60}-poly (N-isopropylacrylamide) block copolymers, *Macromolecules*, 2008, **41**, 7857–7862.

7 H. Huang, B. Chung, J. Jung, H. W. Park and T. Chang, Toroidal micelles of uniform size from diblock copolymers, *Angew. Chem., Int. Ed.*, 2009, **48**, 4594–4597.
8 C. Liu, G. Chen, H. Sun, J. Xu, Y. Feng, Z. Zhang, T. Wu and H. Chen, Toroidal micelles of polystyrene-block-poly (acrylic acid), *Small*, 2011, **7**, 2721–2726.
9 L. Chen, T. Jiang, J. Lin and C. Cai, Toroid formation through self-assembly of graft copolymer and homopolymer mixtures: experimental studies and dissipative particle dynamics simulations, *Langmuir*, 2013, **29**, 8417–8426.
10 X. Xiao, S. He, M. Dan, F. Huo and W. Zhang, Nanoparticle-to-vesicle and nanoparticle-to-toroid transitions of pH-sensitive ABC triblock copolymers by in-to-out switch, *Chem. Commun.*, 2014, **50**, 3969–3972.
11 H. Luo, J. L. Santos and M. Herrera-Alonso, Toroidal structures from brush amphiphiles, *Chem. Commun.*, 2014, **50**, 536–538.
12 J. Cai, K. P. Mineart, X. Li, R. J. Spontak, I. Manners and H. Qiu, Hierarchical self-assembly of toroidal micelles into multidimensional nanoporous superstructures, *ACS Macro Lett.*, 2018, **7**, 1040–1045.
13 L. Hou, W. C. Li, C. Y. Liu, Y. Zhang, W. H. Qiao, J. Wang, D. Q. Wang, C. H. Jin and A. H. Lu, Selective synthesis of carbon nanorings via asymmetric intramicellar phase-transition-induced tip-to-tip assembly, *ACS Cent. Sci.*, 2021, **7**, 1493–1499.
14 G. M. Whitesides and B. Grzybowski, Self-assembly at all scales, *Science*, 2002, **295**, 2418–2421.
15 D. J. Pochan, Z. Y. Chen, H. G. Cui, K. Hales, K. Qi and K. L. Wooley, Toroidal triblock copolymer assemblies, *Science*, 2004, **306**, 94–97.
16 J. Zhu, Y. Liao and W. Jiang, Ring-shaped morphology of "crew-cut" aggregates from ABA amphiphilic triblock copolymer in a dilute solution, *Langmuir*, 2004, **20**, 3809–3812.
17 X. Hong, S. Liu and Y. Wang, Two-dimensional self-assembly of diblock copolymers into nanoscopic aggregates: from dots to disks, then rings, and finally short and long rods, *Soft Matter*, 2013, **9**, 5642–5648.
18 C. Yang, L. Gao, J. Lin, L. Wang, C. Cai, Y. Wei and Z. Li, Toroid formation through a supramolecular "cyclization reaction" of rodlike micelles, *Angew. Chem., Int. Ed.*, 2017, **56**, 5546–5550.
19 R. C. Steinhaus, M. Müllner, T.-L. Nghiem, M. Hildebrandt and A. H. Gröschel, Confinement assembly of ABC triblock terpolymers for the high-yield synthesis of janus nanorings, *ACS Nano*, 2019, **13**, 6269–6278.
20 X. Y. Zhou, C. C. Gao, Y. N. Gao, Y. R. Fan and H. Sun, Polymeric toroids derived from the fusion-induced particle assembly of anisotropic bowl-shaped nanoparticles, *ACS Macro Lett.*, 2023, **12**, 821–827.
21 Z. F. Jia, V. A. Bobrin and M. J. Monteiro, Temperature-directed assembly of stacked toroidal nanorattles, *ACS Macro Lett.*, 2017, **6**, 1223–1227.
22 P. Xu, L. Gao, C. Cai, J. Lin, L. Wang and X. Tian, Helical toroids self-assembled from a binary system of polypeptide homopolymer and its block copolymer, *Angew. Chem., Int. Ed.*, 2020, **59**, 14281–14285.
23 B. Xu, H. Qian and S. Lin, Self-assembly and photoinduced spindle-toroid morphology transition of macromolecular double-brushes with azobenzene pendants, *ACS Macro Lett.*, 2020, **9**, 404–409.
24 J. Zhang, K. Liu, K. Müllen and M. Yin, Self-assemblies of amphiphilic homopolymers: synthesis, morphology studies and biomedical applications, *Chem. Commun.*, 2015, **51**, 11541–11555.
25 S. Basu, D. R. Vutukuri, S. Shyamroy, B. S. Sandanaraj and S. Thayumanavan, Invertible amphiphilic homopolymers, *J. Am. Chem. Soc.*, 2004, **126**, 9890–9891.
26 E. N. Savariar, S. V. Aathimanikandan and S. Thayumanavan, Supramolecular assemblies from amphiphilic homopolymers: testing the scope, *J. Am. Chem. Soc.*, 2006, **128**, 16224–16230.
27 T. S. Kale, A. Klaikherd, B. Popere and S. Thayumanavan, Supramolecular assemblies of amphiphilic homopolymers, *Langmuir*, 2009, **25**, 9660–9670.
28 F. Wang, A. Gomez-Escudero, R. R. Ramireddy, G. Murage, S. Thayumanavan and R. W. Vachet, Electrostatic control of peptide side-chain reactivity using amphiphilic homopolymer-based supramolecular assemblies, *J. Am. Chem. Soc.*, 2013, **135**, 14179–14188.
29 P. Rangadurai, M. R. Molla, P. Prasad, M. Caissy and S. Thayumanavan, Temporal and triggered evolution of host–guest characteristics in amphiphilic polymer assemblies, *J. Am. Chem. Soc.*, 2016, **138**, 7508–7511.
30 J. Z. Du, H. Willcock, J. P. Patterson, I. Portman and R. K. O'Reilly, Self-assembly of hydrophilic homopolymers: a matter of RAFT end groups, *Small*, 2011, **7**, 2070–2080.
31 L. Fan, J. Jiang, Q. Sun, K. Hong, E. J. Cornel, Y. Zhu and J. Du, Homopolymer vesicles with a gradient bilayer membrane as drug carriers, *Chem. Commun.*, 2013, **49**, 11521–11523.
32 T. Liu, W. Tian, Y. Zhu, Y. Bai, H. Yan and J. Du, How does a tiny terminal alkynyl end group drive fully hydrophilic homopolymers to self-assemble into multicompartment vesicles and flower-like complex particles?, *Polym. Chem.*, 2014, **5**, 5077–5088.
33 H. Sun, D. Liu and J. Du, Nanobowls with controlled openings and interior holes driven by the synergy of hydrogen bonding and π–π interaction, *Chem. Sci.*, 2019, **10**, 657–664.
34 L. Fan, J. Jiang, Q. Sun, K. Hong, E. J. Cornel, Y. Zhu and J. Du, Fluorescent homopolypeptide toroids, *Polym. Chem.*, 2022, **13**, 1495–1501.
35 S. R. Mane and R. Shunmugam, Hierarchical self-assembly of amphiphilic homopolymer into unique superstructures, *ACS Macro Lett.*, 2014, **3**, 44–50.
36 J. Zhang, S. You, S. Yan, K. Müllen, W. Yang and M. Yin, pH-Responsive self-assembly of fluorophore-ended homopolymers, *Chem. Commun.*, 2014, **50**, 7511–7513.
37 J. Li, Y. Fan, Q. Gu, X. Zhou, H. Sun and J. Du, Homopolymer self-assembly: principles, driving forces, and applications, *Chem. Mater.*, 2023, **35**, 10348–10370.

38 Y. Zhu, L. Liu and J. Du, Probing into homopolymer self-assembly: how does hydrogen bonding influence morphology?, *Macromolecules*, 2013, **46**, 194–203.
39 H. Qiu, Z. Yang, M. Köhler, J. Ling and F. H. Schacher, Synthesis and solution self-assembly of poly(1,3-dioxolane), *Macromolecules*, 2019, **52**, 3359–3366.
40 F. Du, B. Qiao, T. D. Nguyen, M. P. Vincent, S. Bobbal, S. Yi, C. Lescott, V. P. Dravid, M. O. Cruz and E. A. Scott, Homopolymer self-assembly of poly(propylene sulfone) hydrogels via dynamic noncovalent sulfone–sulfone bonding, *Nat. Commun.*, 2020, **11**, 4896.
41 J. Zhuang, M. R. Gordon, J. Ventura, L. Li and S. Thayumanavan, Multi-stimuli responsive macromolecules and their assemblies, *Chem. Soc. Rev.*, 2013, **42**, 7421–7435.
42 C. Y. Hsu, S. C. Chang, K. Y. Hsu and Y. L. Liu, Photoluminescent toroids formed by temperature-driven self-assembly of rhodamine B end-capped poly(*N*-isopropylacrylamide), *Macromol. Rapid Commun.*, 2013, **34**, 689–694.
43 L. Chen, M. Xu, J. Hu and Q. Yan, Light-initiated in situ self-assembly (LISA) from multiple homopolymers, *Macromolecules*, 2017, **50**, 4276–4280.
44 T. Wu, H. Sun, J. Jiang, S. Lin, L. Fan, K. Hong, Q. Sun, Y. Hu, Y. Zhu and J. Du, Homopolymer nanobowls with a controlled Size and Denting Degree, *Polym. Chem.*, 2022, **13**, 1236–1242.
45 K. Wang, X. Liu, Z. Li, F. Zhao, G. Liu and Y. Zeng, New family of multistimuli-responsive acrylamide-based homopolymers: synthesis, responsive behavior, and application in controlled release, *Macromolecules*, 2025, **58**, 5208–5219.
46 H. Sun, X. Zhou, Y. Leng, X. Li and J. Du, Transformation of amorphous nanobowls to crystalline ellipsoids induced by trans–cis isomerization of azobenzene, *Macromol. Rapid Commun.*, 2022, **43**, 2200131.
47 X. Wang, J. Lu, S. Shi, S. Li, H. Guo, A.-C. Shi and B. Liu, Well-defined homopolymer nanoparticles with uniaxial molecular orientation by synchronized polymerization and self-assembly, *J. Am. Chem. Soc.*, 2024, **146**, 22661–22674.
48 A. Natansohn and P. Rochon, Photoinduced motions in azo-containing polymers, *Chem. Rev.*, 2002, **102**, 4139–4176.
49 D. Wang and X. Wang, Amphiphilic azo polymers: molecular engineering, self-assembly and photoresponsive properties, *Chem. Soc. Rev.*, 2013, **38**, 271–301.
50 M. Zheng and J. Yuan, Polymeric nanostructures based on azobenzene and their biomedical applications: synthesis, self-assembly and stimuli-responsiveness, *Org. Biomol. Chem.*, 2022, **20**, 749–767.
51 Y. Wang, P. Han, H. Xu, Z. Wang, X. Zhang and A. V. Kabanov, Photocontrolled self-assembly and disassembly of block ionomer complex vesicles: a facile approach toward supramolecular polymer nanocontainers, *Langmuir*, 2010, **26**, 709–715.
52 W. Song, X. Qu, Y. Li, J. Li, C. Wang and L. Ding, Azobenzene-containing alternating and random metathesis copolymers toward gaining more insight into photoisomerization properties, *Macromolecules*, 2021, **54**, 9185–9194.
53 Y. Li, W. Song, J. Li, C. Wang and L. Ding, Azobenzene-containing side-chain ionic metathesis polymers: facile synthesis, self-assembly and photoresponsive behavior, *Polymer*, 2021, **232**, 124183.
54 H. Jin, P. Wu, Z. Liu, Z. Sun, W. Feng, Y. Ding, H. Cao, Z. Lin and S. Lin, Robust multifunctional ultrathin 2 nanometer organic nanofibers, *ACS Nano*, 2024, **18**, 21576–21584.
55 W. Li, H. Zhang, Z. Zhai, X. Huang, S. Shang and Z. Song, Fast and reversible photoresponsive self-assembly behavior of rosin-based amphiphilic polymers, *J. Agric. Food Chem.*, 2022, **70**, 12885–12896.
56 P. Xu, L. Gao, C. Cai, J. Lin, L. Wang and X. Tian, Polymeric toroidal self-assemblies: diverse formation mechanisms and functions, *Adv. Funct. Mater.*, 2022, **32**, 2106036.
57 P. Xing, H. Chen, L. Bai, A. Hao and Y. Zhao, Superstructure formation and topological evolution achieved by self-organization of a highly adaptive dynamer, *ACS Nano*, 2016, **10**, 2716–2727.
58 H. Qiu, A. M. Oliver, J. Gwyther, J. Cai, R. L. Harniman, D. W. Hayward and I. Manners, Uniform toroidal micelles via the solution self-assembly of block copolymer–homopolymer blends using a “frustrated crystallization” approach, *Macromolecules*, 2019, **52**, 113–120.